# Active full-shell grazing-incidence optics

Jacqueline M. Roche, Ronald F. Elsner, Brian D. Ramsey, Stephen L. O'Dell,
Jeffrey J. Kolodziejczak, Martin C. Weisskopf, Mikhail V. Gubarev

NASA Marshall Space Flight Center, Astrophysics Office, MSFC/ZP12, Huntsville, AL 35812

## ABSTRACT

MSFC has a long history of developing full-shell grazing-incidence x-ray optics for both narrow (pointed) and wide field (surveying) applications. The concept presented in this paper shows the potential to use active optics to switch between narrow and wide-field geometries, while maintaining large effective area and high angular resolution. In addition, active optics has the potential to reduce errors due to mounting and manufacturing lightweight optics. The design presented corrects low spatial frequency error and has significantly fewer actuators than other concepts presented thus far in the field of active x-ray optics. Using a finite element model, influence functions are calculated using active components on a full-shell grazing-incidence optic. Next, the ability of the active optic to effect a change of optical prescription and to correct for errors due to manufacturing and mounting is modeled.

**Keywords:** x-ray optics, active optics, finite element modeling, opto-mechanical, x-ray telescopes, adaptive optics

## 1. INTRODUCTION

The successes of past missions leads us to demand ever-larger effective areas and finer angular resolutions within manageable launch weights and overall cost budgets. For x-ray astronomy, the overarching requirement is to develop the capability of light-weighting x-ray optics while maintaining high angular resolution for both wide field and narrow field applications. Under current constraints, the same prescription must be used for both wide field and narrow field applications, however, active optics have the potential to switch between a prescription optimized for wide-field angular resolution and a prescription optimized for narrow-field angular resolution. Another advantage of active x-ray optics is the potential to correct manufacturing and mounting errors. This is a significant challenge as reducing the mass of an optic inherently reduces its stiffness, resulting in fabrication- and mounting-induced large deformations of the optical surface. The use of actuators, to modify an optic's shape, can potentially solve this problem [1, 2, 3, 4, 5, 6].

## 2. BACKGROUND

### Technology objectives

MSFC has been developing electroformed nickel optics for a variety of applications for almost 25 years [7, 8]. While such mirrors can be made quite thin to satisfy mass constraints, the lightweight mirrors are more susceptible to figure errors introduced by the replication process and by mounting. One technique to overcome this is differential deposition [9], which uses physical vapor deposition to correct axial figure errors. This technique works well for mid to high spatial-frequency errors, but is not well suited to low frequencies, where typically large amounts of material must be deposited. The technique proposed here has a limited number of actuators and can address these low-frequency errors.

The Spectrum-Rontgen-Gamma mission has an all-sky-survey followed by a pointed-observations phase [10]. For the former, a wide-field prescription is desirable, whereas for the latter, a narrow-field prescription, which optimizes on-axis angular resolution, is required. Typically, missions must compromise between the two. In the case of the ART-XC instrument aboard SRG, the MSFC-fabricated optics were purposely de-focused slightly, improving off-axis performance at the expense of on-axis [11]. Clearly, the ability to switch, on-orbit between the two prescriptions, would be highly desirable.

## Optical deformable mirrors

Deformable mirrors (DMs) were developed mainly by the military but emerged as a reliable component in optical astronomy in the 1990s [12]. Traditional DMs have a square grid of actuators normal to the back surface of an optic. The combination of the gaussian shapes each actuator creates on the mirror surface corrects for distortions in the atmosphere in real time. The impact of adaptive optics in astronomy is shown in Figure 1. An image of distant galaxies is taken with and without adaptive optics at the Keck Observatory, showing a remarkable improvement in resolution.

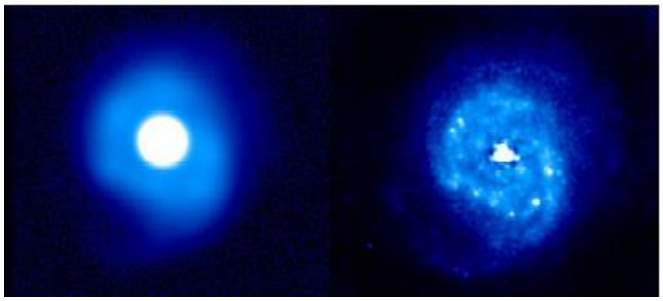

**Figure 1**: Image at Keck Observatory of a distant galaxy with (right) and without (left) adaptive optics.

In the early 2000's Northrop Grumman AOA Xinetics (NG AOA/Xinetics) developed the zonal meniscus DM, a lightweight deformable mirror for space-based adaptive optics, using a CERAFORM silicon carbide structure with a reflective front surface and stacked lead magnesium niate (PMN) electrostrictive actuators. The DM design integrates the PMN actuators into the ribs of a lightweighted SiC structure, parallel to the optic, creating modal shape changes across the surface of the optic [13]. The PMN is a highly electrostrictive, ferroelectric ceramic material that can be optimized for displacement and hysteresis over a desired operating temperature range [14]. In 2010, NG AOA/Xinetics developed a DM with an even lower areal density called a surface-parallel array (SPA) DM, which uses its patented multi-channel surface-parallel zonal transducer system [15]. The entire transducer contains all individually addressable components and is bonded directly to the back of an optical membrane. The actuation runs parallel to the membrane, creating a moment on the back of the optic similar to the zonal meniscus-type deformable mirror. The SPA DM also uses stacked PMN actuation [16].

## X-ray active optics

In response to the mandate for high effective area and high angular resolution, the Smithsonian Astrophysical Observatory (SAO) developed a concept of using pixelated active components on segmented grazing-incidence optics. The concept contains 8400 segments, creating 292 nested shells. Each segment has a thin film of piezoelectric material deposited on the back of an extremely thin mirror, with a 40x40 active grid of 1600 individually addressable actuators. With 1600 actuators on each segment and 8400 segments, the resulting $10^7$ active components adds a lot of complexity to an already complex design [15, 16, 17].

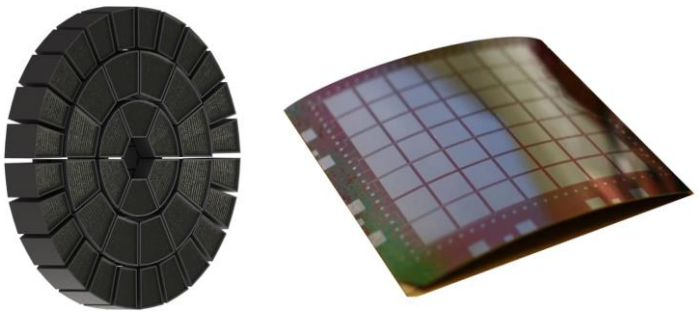

**Figure 2**: Left: SAO concept for a segmented active x-ray optic, 8400 segments. Right: SAO concept for actuator is bimorph array on each segment. Shown with a 7x7 PZT array, which will be scaled to 40x40 PZT, totaling $10^7$ active components [17].

NG AOA/Xinetics partnered with SAO to apply their SPA actuation to a grazing-incidence optic using a 15mm spacing. When applied to the SAO concept shown in Figure 2, each segment would have approximately 850 actuators, totaling $7x10^6$ actuators. Using a finite element model of a grazing-incidence optic, the SPA actuation corrects 99% of the P-V input error with a majority of the residual error at the edges of the segment. The model is done without edge supports, and the addition of mounts will increase error at the edge of the optic. However, the use of surface-normal actuators at each mount position could decrease the errors due to mounting. However, adjusting at least four mounts on each of 8400 segments is 33,600 active mounts in addition to the $7x10^6$-$10^7$ adjustable parts of the design [15, 18, 19, 20].

Although the concepts for active x-ray optics show potential to correct high- to mid-spatial frequencies, the number of actuators to control, plus, the number active mounts makes the already complex concept of an 8400 segmented x-ray optic even more daunting. Targeting the low-spatial frequency shape changes on full-shell optics will drastically reduce the number of components in the active x-ray optic. The correction of manufacturing and mounting errors can be done in conjunction with differential deposition, which targets the high- to mid-spatial frequencies. Correcting low-spatial frequency also lends itself to making prescription changes in the full-shell optic.

## 3. ACTIVE FULL-SHELL GRAZING-INCIDENCE OPTIC CONCEPT

### Active optics for prescription change

At MSFC, we are investigating the concept of using active optics to switch between an optimized wide field prescription and an optimized narrow-field prescription. Adjusting an x-ray telescope in space would enable an all-sky mission to be done with the same telescope as a pointed mission without sacrificing the angular resolution for the wide field or the narrow field.

As shown in Figure 3, the angular resolution of the x-ray prescription varies as a function of the field angle. The plot is conceptual, showing a prescription optimized for a narrow field in red and a prescription optimized for a wide field in blue. The red line shows a high angular resolution at a narrow field but degrades quickly when moving off-axis. The blue line has a lower angular resolution in the narrow field but maintains a similar resolution in the wide field.

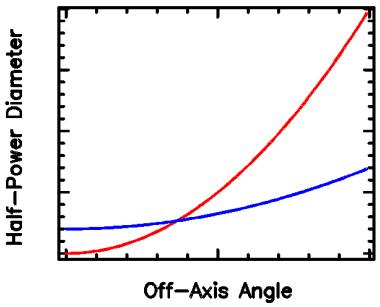


**Figure 3**: X-ray optical prescription design space; red=example of an optimized narrow-field prescription (potentially Wolter Schwarzchild), blue=example of an optimized wide-field prescription (potentially polynomial prescription)

### Wolter I to Wolter Schwarzchild

As the design of a wide field polynomial prescription is in progress, the concept of adjusting the shell between two prescriptions will be demonstrated using the Wolter I and the Wolter Schwarzchild prescriptions. In reality, because the Wolter Schwarzchild performs better than the Wolter I off-axis and performs as well as the Wolter I prescription on-axis, there is no benefit in switching between these two particular prescriptions. However, for demonstration purposes, we will present this prescription change as indicative of the shape changes that can be effected [21, 22].

Figure 4 shows the difference in prescriptions between the Wolter Schwarzchild and the Wolter I x-ray telescopes, for 6 shells with dimensions loosely based on a concept for the X-ray Surveyor mission. The focal length is 10 m, the mirror segment length is 0.4 m, the shell thickness is 0.001 m, and the nested shell diameters vary from 0.5 m and 1 m. The geometric areas of the Wolter I and Wolter Schwarzchild telescopes with identical focal lengths and intersection radii will be slightly different. Since the area will remain constant in the case of an active optic switching between the two prescriptions, the parameters for the Wolter Schwarzchild were adjusted using a method introduced by Chase and VanSpeybroek to maintain the same geometric area as the Wolter I [21, 22].

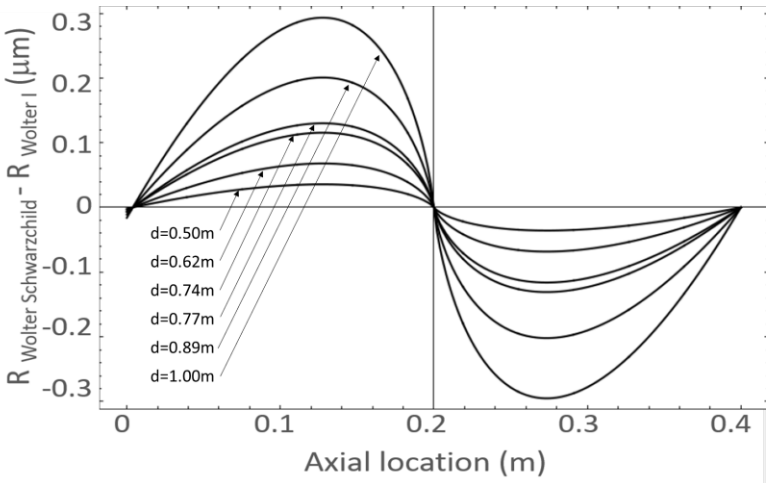


**Figure 4**: Radius difference between Wolter Schwarzchild and Wolter I prescriptions for six nested shells with diameters=0.5-1.0m, focal length=10m, length=0.4m, and thickness=0.001m.

Figure 4 shows the difference between the Wolter Schwarzchild and Wolter I has a low-spatial frequency and is less than 0.3 μm in amplitude. An optimization tool was developed to determine a point design for the active optics analysis. It can create models of nested full-shells with varying parameters. For simplicity only one shell will be used to demonstrate the capability of switching from a Wolter I prescription to a Wolter Schwarzchild prescription.

### Optical DMs applied to active x-ray optics

In order to apply the optical DM technology to x-ray optics, the actuation schemes discussed in Section 2 are applied to the full-shell grazing-incidence optic. Figure 5 shows the concept of applying the surface-normal, zonal meniscus, and SPA actuators to a full shell. Using the surface-normal actuators, the entire surface of an x-ray optic is propagated, creating a higher areal density, larger obscuration of the aperture and more complexity. The zonal meniscus actuation would not require as much areal density or complexity as the surface-normal actuation, but the ribs required on the back of the optic would obscure too much light for nested x-ray optics. Both surface-normal and surface-parallel actuators obscure a large percentage of the aperture. Plus, both types of actuation must be individually wired, requiring even more space and complexity.

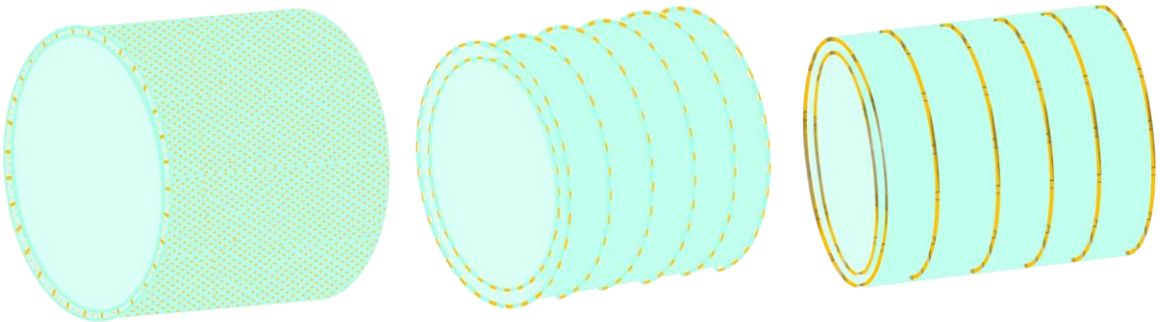

**Figure 5**: Left: side view of surface-normal actuators between 2 nested full-shell x-ray optics. Center: Side view of zonal-meniscus actuators on 2 nested full-shell x-ray optic. Right: Side view of SPA on 2 nested full-shell x-ray optic.

The concept presented in this paper applies the SPA actuation to full-shell grazing-incidence optics, because it minimizes the areal density, the obscuration and the complexity of the active optic.

### Point design

A point design (shown in Figure 6) was developed by applying the SPA actuation to a one meter Wolter I shell with a focal length of 10 m, a length of 0.4 m, and a thickness of 0.001. It was optimized to create low spatial frequency changes, specifically to change the one meter Wolter I prescription to a Wolter Schwarzchild prescription, shown in Figure 4.

In order to create low-spatial frequencies on the full-shell optics, actuation is applied circumferentially in a surface parallel direction, with the SPA actuators in a band around the shell. As opposed to the NG AOA/Xinetics DM with a hexagagonal pattern, the ceramic wafers are stacked in line with one another. The diode in between the active sections, allows each section to be individually addressable without individual wiring. The resulting shape of the actuation is a slope change in the longitudinal direction.

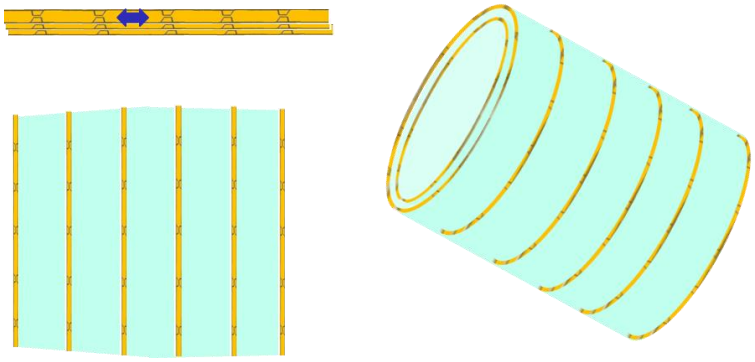

**Figure 6**: Active full-shell concept. Top left: stacked layers of PMN wafers with electrodes in between each section, individually addressable. Bottom left: side view of SPA technology applied to full-shell optics. Right: full view of point design.

### Fabrication and mounting Errors

Although we optimized the concept for the prescription change, we also investigated how well it corrects for manufacturing and mounting errors. Shell fabrication does produce some low-order errors, as seen in Figure 7. However, mounting errors are localized.

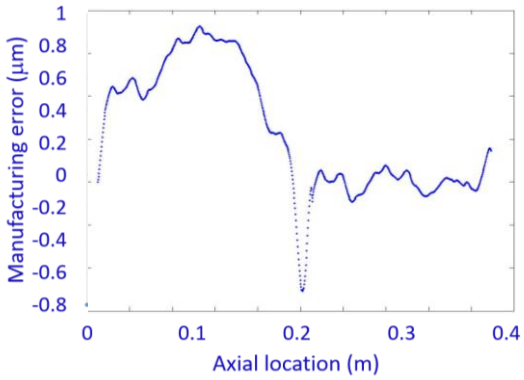


**Figure 7**: Manufacturing error of a full-shell grazing-incidence optic (μm)

Results of correcting the error shown in Figure 7 will be presented in Section 5. The point design can correct for low-frequency errors but not mid- and high-frequencies. It is thus complementary to differential deposition, which is a viable approach for correcting mid-to-high-frequency errors.

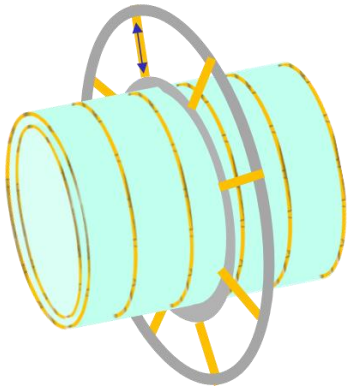

**Figure 8**: Utilizing the concept of using surface-normal actuators for adjustable mounts, errors due to mounting can be reduced.

The point design discussed in depth in this paper is not conducive to correct the localized errors from mounting, however, surface-normal actuation can be used in conjunction with the current point design to minimize these errors. Developing an active mount can potentially reduce the effects of mounting the optic. This concept is shown in Figure 8. Because the location of errors due to mounting significantly effects its angular resolution [24], and it also effects the influence of the actuators, the location of a mount for an active optic must be optimized. For simplicity, the point design has a mount at the center of the shell.

## 4. FINITE ELEMENT ANALYSIS

A finite-element model (FEM) of the point design discussed in Section 3 was built using ANSYS software (shown in Figure 9). Thin shell elements were used to model both the grazing-incidence optic and the actuators. For the sake of this study, we use beryllium aluminum for the optic (shown in blue), because we're investigating it for future optics. The surface parallel bands are made of stacked PMN, shown in gold. The mount is simplified by holding the center of the shell (shown in pink) at a zero displacement.

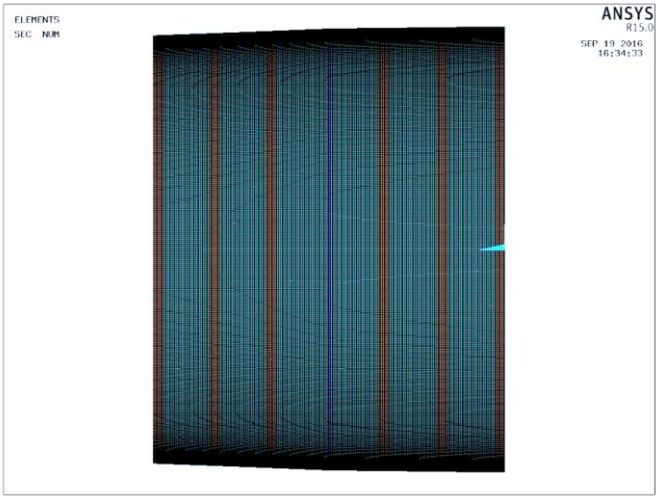


**Figure 9**: Finite element model; blue=beryllium aluminum, yellow=PMN bonded to beryllium aluminum, purple=simplified mount (zero displacement)

In order to determine the influence of each actuator on the optical surface of the shell (the influence function), the expansion of the actuator is applied as a thermal load, representing the equivalent of one micron of stroke in the actuator. Because the SPA band actuation is conceptual, its stroke is unknown and awaits more definitive specifications. The resulting deformation on the optical surface is exported to a text file. Figure 10 shows an influence function of an actuator.

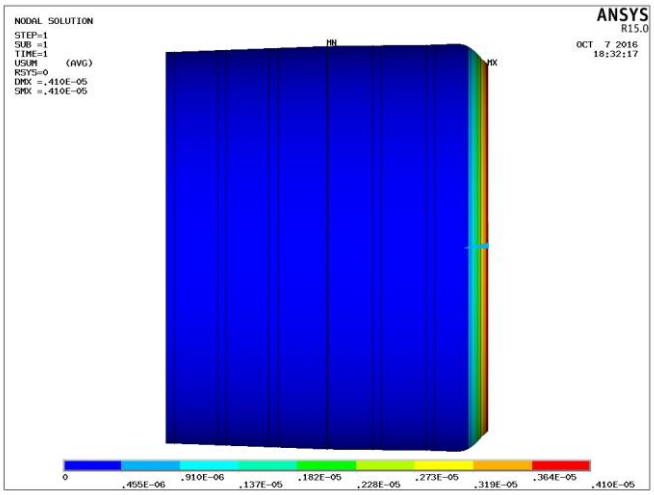


**Figure 10**: Resulting influence function on the optical surface (in meters) from 1μm of stroke on the edge SPA band on a 1m diameter full-shell Wolter I optic

The images in Figure 11 show the displacement of each influence function.

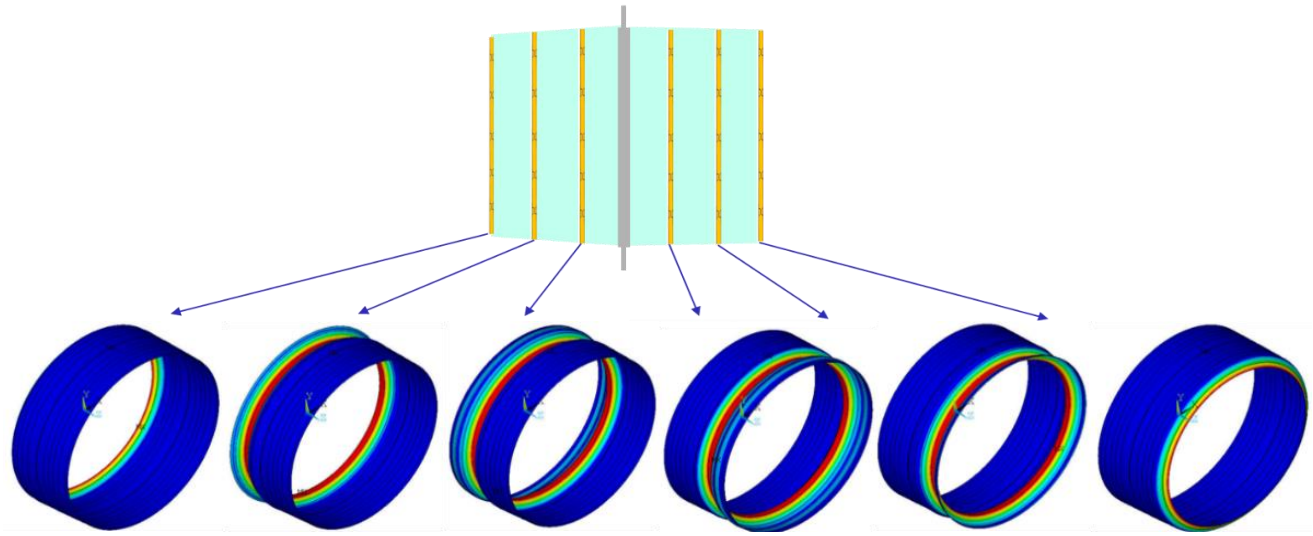

**Figure 11**: Normalized influence functions in FEM, resulting from load on each actuator

The resulting deformation on the optical surface is exported to a text file for each actuator; this is used to analyze how well it corrects for a given shape. The influence functions are imported into MATLAB, and a least square fit to the desired shape is performed to determine the actuated shape. Currently, the performance of the full-shell active optic is analyzed using the surface root mean square (RMS). The next phase of the analysis will include analyzing the error in the surface slope data.

## 5. RESULTS

### Prescription change

The point design of the Wolter I optic discussed in Section 3 was analyzed to determine its capability of changing shapefrom a Wolter-I prescription to a Wolter Schwarzchild prescription. The difference between the prescriptions is show in Figure 4. Using MATLAB, the influence functions imported from the FEM of the point design are fit to the difference between the Wolter Schwarzchild prescription and the Wolter I prescription. The metric used to show the capability of the active optic to correct a specific shape is called correctability, shown in Figure 12.

$$\text{correctability} = \frac{(\text{RMS}_{\text{desired shape}} - \text{RMS}_{\text{calculated shape}})}{\text{RMS}_{\text{desired shape}}}$$

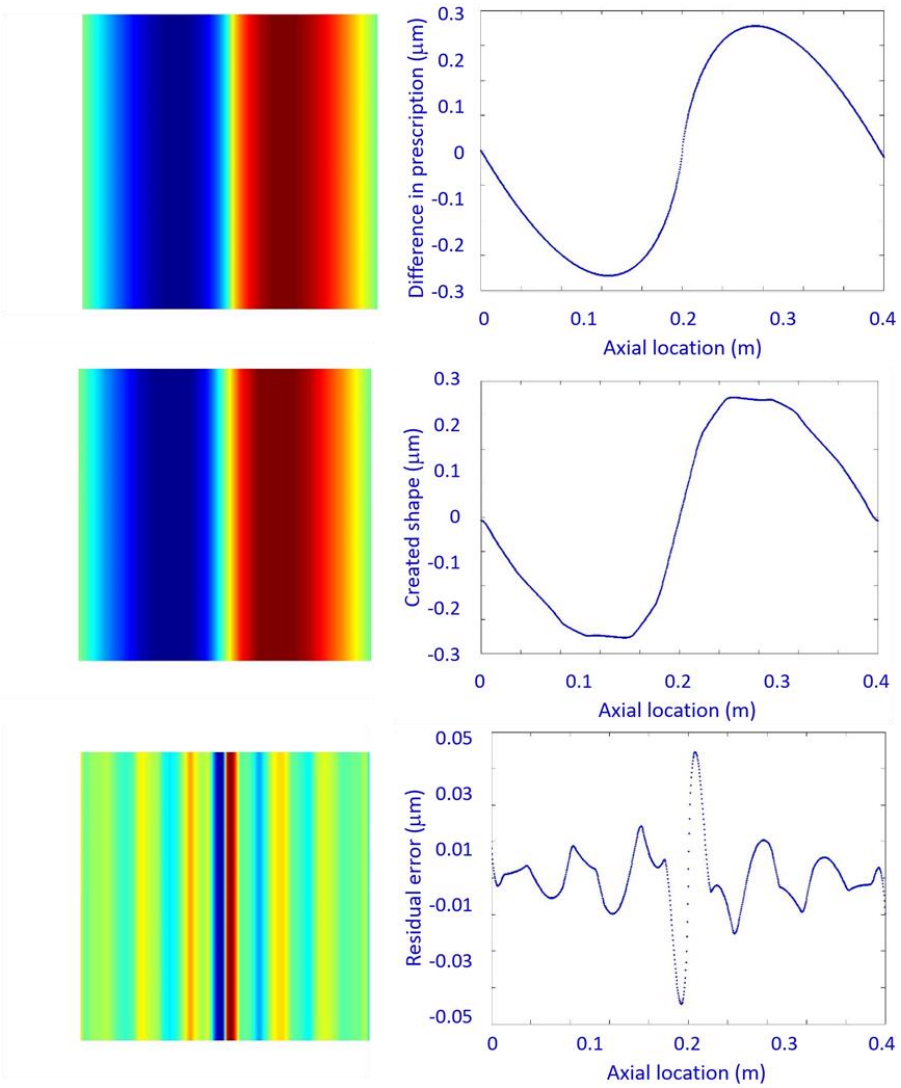


**Figure 12**: Top: desired prescription change in optical surface (μm). Middle: resulting shape change in optical surface based on FEM results (μm). Bottom: residual surface error between the desired and calculated shapes (μm).

The point design corrects to 92% of the desired surface RMS amplitude. An assessment is underway to compare the achieved angular resolution, factoring in residual slope errors, as a function of off-axis angle for the two prescriptions.

### Manufacturing errors

Figure 13 shows the correction of the fabrication errors discussed in Section 3. Using the same method as above, the correctability of the fabrication errors are 68% surface RMS height but did not significantly improve the slope RMS, which is dominated by higher frequencies than those addressed by the small number of actuators used.

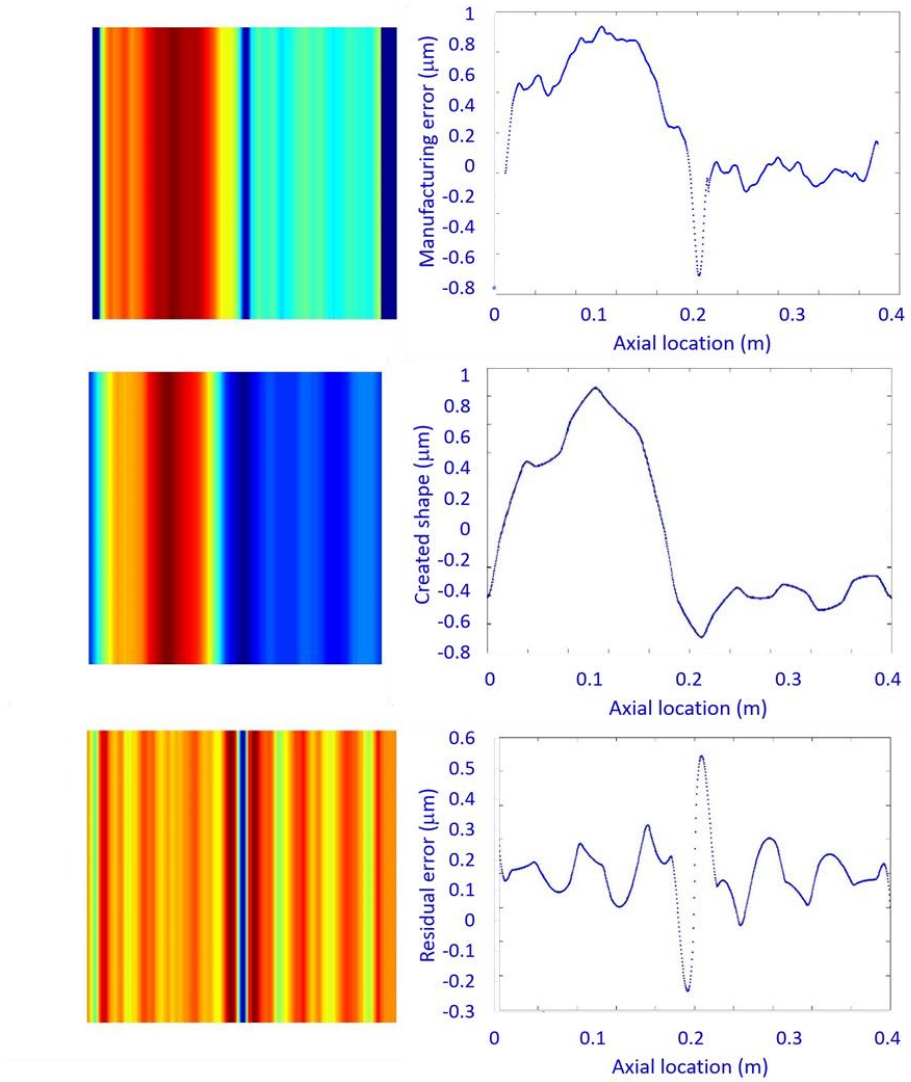


**Figure 13**: Top: manufacturing error on optical surface (μm). Middle: resulting shape change on optical surface based on FEM results (μm). Bottom: residual surface error between the desired and calculated shapes (μm).

## 6. SUMMARY

The analytical results in this paper prove the concept of active full-shell grazing-incidence optics as a viable technology to adjust the optical prescription in space, switching from a wide to narrow field instrument. This potentially offers significant benefits as an all-sky survey is essential to discovering new x-ray sources, and a pointing mission is necessary to understand the sources. Thus far in x-ray astronomy, the angular resolution for either wide field or the narrow field was sacrificed for the benefit of the other.

The design chosen for this paper is shown to correct for low-order spatial shape changes in the full-shell optic, which also lends itself to correcting for low-spatial frequency errors in the optic along with prescription change. Corrective polishing and differential deposition are viable ways to correct for mid- to high- spatial frequencies, however most manufacturing errors span the full spatial frequency range.

Moving forward, the wide field prescription must be optimized, the active shell must be adapted to the new prescription change, and the circumferential correction of the active shell must be analyzed. In parallel, the multichannel arrays must be adapted to circular bands, and the true influence functions must be tested.

## 7. REFERENCES


[1] Weisskopf, M.C., Aldcroft, T.L., Bautz, M., Cameron, R.A., Dewey, D., Drake, J.J, Grant, C.E., Marshall, H.L., and Murray, S.S, "An Overview of the Performance of the Chandra X-ray Observatory," Exp. Astron. 16, 1–68 (2003).

[2] Weisskopf, M.C., Brinkman, B., Canizares, C., Garmire, G., Murray, S., and Van Speybroeck, L.P., "An Overview of the Performance and Scientific Results from the Chandra X-Ray Observatory," Pub. Astron. Soc. Pac. 114, 1–24 (2002).

[3] Weisskopf, M.C., Tananbaum, H.D., Van Speybroeck, L.P., and O'Dell, S.L., "Chandra X-ray Observatory (CXO): overview," Proc. SPIE 4012, 2–16 (2000).

[4] Aschenbach, B., Briel, U.G., Haberl, F., Braeuninger, H. W., Burkert, W., Oppitz, A., Gondoin, P. and Lumb, D.H., "Imaging performance of the XMM-Newton x-ray telescopes," Proc. SPIE 4012, 731-739 (2000).

[5] Jansen, F., Lumb, D., Altieri, B., Clavel, J., Ehle, M., Erd, C., Gabriel, C., Guainazzi, M., Gondoin, P., Much, R., Munoz, R., Santos, M., Schartel, N., Texier, D. and Vacanti, G., "XMM-Newton observatory. I. The spacecraft and operations," Astron. and Astrophys. 365, L1-L6 (2001).

[6] Aschenbach, B., "In-orbit performance of the XMM-Newton x-ray telescopes: images and spectra," Proc. SPIE 4496, 8-22 (2002).

[7] Ramsey, B.D., Atkins, C., Gubarev, M.V., Kilaru, K., O'Dell, S.L., "Optics requirements for x-ray astronomy and developments at the Marshall Space Flight Center," Nuclear Instruments and Methods in Physics Research A 616, 110 (2012).

[8] Ramsey, B.D., Atkins, C., Gubarev, M.V., Kilaru, K., O'Dell, S.L., "Optics requirements for x-ray astronomy and developments at the Marshall Space Flight Center," Nuclear Instruments and Methods in Physics Research A 616, 110 (2012).

[9] Kilaru K, Ramsey BD, Gubarev MV, Gregory DA, "Differential deposition technique for figure corrections in grazing-incidence x-ray optics," Opt. Eng. 50(10), 106501 (September 28, 2011).

[10] M. Pavlinsky, V. Akimov, V. Levin, A. Krivchenko, A. Rotin, M. Kuznetsova, I. Lapshov, A. Tkachenko, N. Semena, M. Buntov, A. Glushenko, V. Arefiev, A. Yaskovich, S. Grebenev, S. Sazonov, M. Revnivtsev, A. Lutovinov, S. Molkov, R. Krivonos, D. Serbinov, M. Kudelin, T. Drozdova, S. Voronkov, R. Sunyaev, E. Churazov, M. Gilfanov, V. Babyshkin, I. Lomakin, A. Menderov, M. Gubarev, B. Ramsey, K. Kilaru, S. L. O'Dell, J. Kolodziejczak, R. Elsner, V. Zavlin, D. Swartz, "Status of ART-XC/SRG instrument," Proc. SPIE 9905, Space Telescopes and Instrumentation 2016: Ultraviolet to Gamma Ray, 99051J (July 18, 2016).

[11] M. Gubarev, B. Ramsey, J. J. Kolodziejczak, S. L. O'Dell, R. Elsner, V. Zavlin, D. Swartz, M. Pavlinsky, A. Tkachenko, I. Lapshov, "The calibration of flight mirror modules for the ART-XC instrument on board the SRG mission," Proc. SPIE 9144, Space Telescopes and Instrumentation 2014: Ultraviolet to Gamma Ray, 91444U (July 28, 2014);

[12] Ealey, M.A., Wellman, J.A. "Xinetics low-cost deformable mirrors with actuator replacement cartridges," Proc. SPIE 2201, Adaptive Optics in Astronomy, 680 (May 31, 1994).

[13] M.A. Ealey, J.A. Wellman, "Highly adaptive integrated meniscus primary mirrors," Proc. SPIE 5166, UV/Optical/IR Space Telescopes: Innovative Technologies and Concepts, 165 (January 30, 2004).

[14] Delgado M, "Phase Transitions in Relaxor Ferroelectrics," http://guava.physics.uiuc.edu/~nigel/courses/563/Essays_2005/PDF/delgado.pdf (December 13, 2005).

[15] Charles F. Lillie, Jeff L. Cavaco, Audrey D. Brooks, Kevin Ezzo, David D. Pearson, John A. Wellman, "Adaptive x-ray optics development at AOA-Xinetics," Proc. SPIE 8777, Damage to VUV, EUV, and X-ray Optics IV; and EUV and X-ray Optics: Synergy between Laboratory and Space III, 877717 (May 3, 2013).

[16] D. Pearson, J. Cavaco, J. Roche, "Multichannel, surface parallel, zonal transducer system," United States Patent 7683524 B2 (March 1, 2007).

[17] Martin C. Weisskopf, Jessica Gaskin, Harvey Tananbaum, Alexey Vikhlinin, "Beyond Chandra: the x-ray Surveyor," Proc. SPIE 9510, EUV and X-ray Optics: Synergy between Laboratory and Space IV, 951002 (May 12, 2015).

[18] Paul B. Reid, Robert A. Cameron, Lester Cohen, Martin Elvis, Paul Gorenstein, Diab Jerius, Robert Petre, William A. Podgorski, Daniel A. Schwartz, William W. Zhang, "Constellation-X to Generation-X: evolution of large collecting area moderate resolution grazing incidence x-ray telescopes to larger area high-resolution adjustable optics," Proc. SPIE 5488, UV and Gamma-Ray Space Telescope Systems, 325 (October 11, 2004).

[19] Charles Lillie, Richard Egan, Franklin Landers, Jeffrey Cavaco, Kevin Ezzo, Ali Khounsary, “Test results for an AOA-Xinetics grazing incidence x-ray deformable mirror,” Proc. SPIE 9208, Adaptive X-Ray Optics III, 92080C (September 17, 2014).

[20] P.B. Reid, T.L. Aldcroft, V. Cotroneo, W. Davis, R.L. Johnson-Wilke, S. McMuldroch, B.D. Ramsey, D.A. Schwartz, S. Trolier-McKinstry, A. Vikhlinin, H. Rudeger, R.H.T Wilke, “Technology development of adjustable grazing incidence x-ray optics for sub-arc second imaging,” Proc. SPIE 8443, 29 (2012).

[21] Paul B. Reid, Thomas L. Aldcroft, Ryan Allured, Vincenzo Cotroneo, Raegan L. Johnson-Wilke, Vanessa Marquez, Stuart McMuldroch, Stephen L. O'Dell, Brian D. Ramsey, Daniel A. Schwartz, Susan E. Trolier-McKinstry, Alexey A. Vikhlinin, Rudeger H. T. Wilke, Rui Zhao, “Development status of adjustable grazing incidence optics for 0.5 arcsecond x-ray imaging,” Proc. SPIE 9208, Adaptive X-Ray Optics III, 920807 (October 3, 2014).

[22] L. P. VanSpeybroeck and R. C. Chase, "Design Parameters of Paraboloid-Hyperboloid Telescopes for X-ray Astronomy," Appl. Opt. 11, 440-445 (1972).

[23] R. C. Chase and L. P. VanSpeybroeck, "Wolter-Schwarzschild Telescopes for X-Ray Astronomy," Appl. Opt. 12, 1042-1044 (1973).

[24] Roche, J. M., Kolodziejczak, J. L., O’Dell, S. L., Elsner, R. F., Weisskopf, M. C., Ramsey, B. D., and Gubarev, M. V., “Opto-mechanical analyses for performance optimization of lightweight grazing-incidence mirrors,” Proc. SPIE 8861, 48 (2013).